

# The fluid–fluid interface in a model colloid–polymer mixture: Application of grand canonical Monte Carlo to asymmetric binary mixtures

R. L. C. Vink and J. Horbach

*Institut für Physik, Johannes Gutenberg-Universität, D-55099 Mainz, Staudinger Weg 7, Germany*

(Dated: October 17, 2003)

We present a Monte Carlo method to simulate asymmetric binary mixtures in the grand canonical ensemble. The method is used to study the colloid–polymer model of Asakura and Oosawa. We determine the phase diagram of the fluid–fluid unmixing transition and the interfacial tension, both at high polymer density and close to the critical point. We also present density profiles in the two–phase region. The results are compared to predictions of a recent density functional theory.

PACS numbers: 61.20.Ja, 64.75.+g

In colloid experiments, hard–sphere–like systems can be realized in which the corresponding phase behavior is of purely entropic origin. An example is the fluid–fluid unmixing transition that is observed in solutions of colloids and non–adsorbing polymers [1, 2]. This transition is due to a depletion effect [1, 2, 3, 4, 5]. Each colloidal particle is surrounded by a depletion zone from which polymers are excluded. When two colloids are close together, their depletion zones may overlap, thereby increasing the free volume available to the polymers. This results in an anisotropic pressure exerted by the polymers onto the colloids which gives rise to an effective attraction between the colloids. Such depletion forces also occur in mixtures of large and small hard spheres, but in this case it is still debated whether phase separation occurs [6].

A simple model for colloid–polymer mixtures was first introduced by Asakura and Oosawa [1] and later independently by Vrij [2]. In this model (the so–called AO model) colloids and polymers are treated as spheres with respective radii  $R_c$  and  $R_p$ . Hard sphere interactions are assumed between colloid–colloid (cc) and colloid–polymer (cp) pairs, while polymer–polymer (pp) pairs can interpenetrate freely. This yields the following pair potentials for the AO model:

$$\begin{aligned} u_{cc}(r) &= \begin{cases} \infty & \text{for } r < 2R_c \\ 0 & \text{otherwise,} \end{cases} \\ u_{cp}(r) &= \begin{cases} \infty & \text{for } r < R_c + R_p \\ 0 & \text{otherwise,} \end{cases} \\ u_{pp}(r) &= 0, \end{aligned} \quad (1)$$

where  $r$  is the distance between two particles. The polymers thus represent ideal polymer coils with a radius of gyration  $R_p$  which can be realized experimentally in a  $\theta$  solvent.

The AO model has been the subject of many studies in the framework of density functional theories (DFT) [7, 8, 9]. In particular, these studies yielded the phase diagram for a wide range of colloid to polymer size ratios. Moreover, in the case of the fluid–fluid unmixing transition, they predicted interfacial tensions that are roughly one thousand times lower than those for simple liquids, in

agreement with experiments [10, 11]. A drawback of the latter DFTs is that they are mean field theories and thus cannot recover the 3D Ising critical behavior observed, for instance, in a recent experiment on a real colloid–polymer mixture [11].

Monte Carlo simulations are also well suited to study the phase behavior of colloid–polymer mixtures. Recent simulations in the Gibbs ensemble were performed to determine phase diagrams of the AO model [12] and also of a model that considers non–zero interactions between the polymers [13]. In the latter study even quantitative agreement with experiments was obtained. However, interfaces are absent in the Gibbs ensemble [14], so these simulations do not enable investigations close to the critical point, nor investigations of the interface in the two–phase region.

The general problem in the simulation of asymmetric binary mixtures (such as the AO model) is that, by displacing or inserting a large particle, overlap with a number of small particles will likely result. Such overlaps are generally unfavorable and will be rejected in the majority of cases. If no special steps are taken, one ends up displacing mainly small particles while the large particles remain essentially frozen. For asymmetric binary mixtures in the canonical ensemble a number of specialized algorithms have been developed that circumvent this problem [15, 16]. Unfortunately, it is difficult to obtain the surface tension accurately in the canonical ensemble because it must be derived from the rather small anisotropy of the pressure tensor in that case: long wavelength interfacial fluctuations are hard to equilibrate in the canonical ensemble [17].

In this letter we present a grand canonical Monte Carlo method that enables direct simulations of asymmetric binary mixtures. We use the method to study the fluid–fluid unmixing transition in the AO model. Our method consists of collective Monte Carlo moves in conjunction with an umbrella sampling technique that was recently developed by Virnau and Müller [18]. This way, we are able to calculate the phase diagram of the AO model close to the critical point. At the same time we can calculate the interfacial tension  $\gamma$  in the two–phase region using

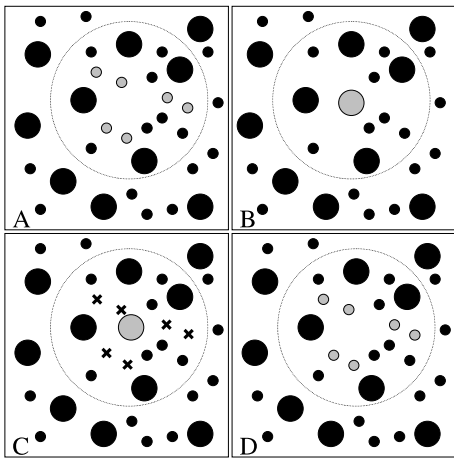


FIG. 1: Schematic picture of the grand canonical Monte Carlo moves used in our simulations. Particles to be inserted or removed are shaded grey. See text for details.

the method of Binder [19]. We present a comparison of our data to recent DFT results [8, 9, 20] and we show that the AO model displays 3D Ising critical behavior.

The grand canonical ensemble requires that the temperature  $T$ , the volume  $V$  and the respective chemical potentials  $\{\mu_p, \mu_c\}$  of the small (polymer) and large (colloid) particles are fixed. In a standard grand canonical move one tries to insert or remove a particle using Metropolis sampling [21]. This approach is not efficient for asymmetric binary mixtures because the insertion of large particles (colloids) is severely hampered by the presence of small particles (polymers). The method that we present is aimed to circumvent this problem. The main idea is to not transfer particles one-at-a-time, but to swap clusters of small particles instead. This stimulates the formation of voids, in which a large particle can be inserted without producing overlap.

Figs. 1A and 1B demonstrate the insertion of an additional large particle into an asymmetric binary mixture currently containing  $N_c$  large particles. First, a point is selected randomly in the mixture and a sphere with radius  $\delta$  and volume  $V_\delta = 4\pi\delta^3/3$  is drawn around it (see Fig. 1A). Let  $n_p$  denote the number of small particles inside the sphere: a particle is inside the sphere when the coordinates of its center are inside the sphere. Next, we choose a uniform random integer  $n_r$  from the interval  $0 \leq n_r < m$ , with  $m$  an integer that will be specified later. If  $n_r > n_p$  the move is rejected but if  $n_r \leq n_p$ ,  $n_r$  small particles are randomly selected from the sphere out of the  $n_p$  present (these particles are shaded grey in Fig. 1A). The  $n_r$  selected particles are then removed from the mixture and a large particle is inserted at the center of the sphere (see Fig. 1B). The new configuration is accepted with probability:

$$A_+ = \min \left[ 1, \frac{z_c V}{N_c + 1} \frac{(n_p)!}{(n_p - n_r)!} \frac{e^{-\beta \Delta E}}{(z_p V_\delta)^{n_r}} \right], \quad (2)$$

with  $\Delta E$  the potential energy difference between the initial and the final configuration and  $\{z_c, z_p\}$  the fugacity of large and small particles, respectively. The fugacity  $z$  is related to the chemical potential via  $z = \exp(\beta\mu)$  with  $\beta = 1/(k_B T)$  and  $k_B$  the Boltzmann constant.

The reverse move is illustrated in Figs. 1C and 1D. First, a large particle is selected at random and a sphere with radius  $\delta$  is drawn around the center of this particle. Next, a uniform random integer  $n_r$  from the interval  $0 \leq n_r < m$  is chosen followed by the selection of  $n_r$  random locations inside the sphere. These random locations are marked as crosses in Fig. 1C. The selected large particle is now removed from the mixture and  $n_r$  small particles are placed on the locations selected before (the newly inserted particles are shaded grey in Fig. 1D). The new configuration is accepted with probability:

$$A_- = \min \left[ 1, \frac{N_c}{z_c V} \frac{(n_p)! (z_p V_\delta)^{n_r}}{(n_p + n_r)!} e^{-\beta \Delta E} \right], \quad (3)$$

the notation being the same as in Eq. (2).

It is straightforward to show that the acceptance probabilities  $A_+$  and  $A_-$  enforce detailed balance, which ensures that the algorithm is not statistically biased [22]. The algorithm is also ergodic because single large particles have a finite probability of being inserted anywhere in the system with one move. Similarly, a small particle can be inserted anywhere via a combination of moves: for example, by the insertion of a large particle followed by the removal of the same large particle.

In order to apply the method to the AO model, the parameters  $\delta$  and  $m$  still need to be specified. We use  $\delta = R_c + R_p$  which is just big enough to contain one colloid in a sea of polymers. The integer  $m$  must be chosen large enough to allow for the formation of voids. In the pure polymer phase, the polymer density equals  $z_p$  because the polymers behave like an ideal gas. The insertion sphere will then contain  $z_p V_\delta$  polymers on average and thus we choose  $m$  slightly above this value. With this choice of  $\delta$ , the insertion of a colloid can only succeed if all polymers are removed from the insertion sphere  $V_\delta$ . This will in general happen a fraction  $1/m$  of the time. To boost the acceptance rate, we choose to remove *all* polymers from  $V_\delta$  when we attempt to insert a colloid, provided their number does not exceed  $m$ : moves that attempt to remove more than  $m$  polymers are rejected. To maintain detailed balance, the acceptance probabilities  $A_+$  and  $A_-$  must be multiplied by  $1/m$  and  $m$ , respectively.

The phase diagram of the AO model can be expressed in terms of the reduced polymer packing fraction  $\eta_p^r \equiv (4\pi/3)z_p R_p^3$  as a function of the colloid packing fraction  $\eta_c \equiv (4\pi/3)R_c^3 N_c/V$ . This is analogous to the temperature–density phase diagram for simple fluids. In case of the AO model,  $\eta_p^r$  plays the role of inverse temperature and  $\eta_c$  that of order parameter. In order to determine the coexistence curve of the fluid–fluid unmixing transition, we calculate for a given value of  $\eta_p^r$  the

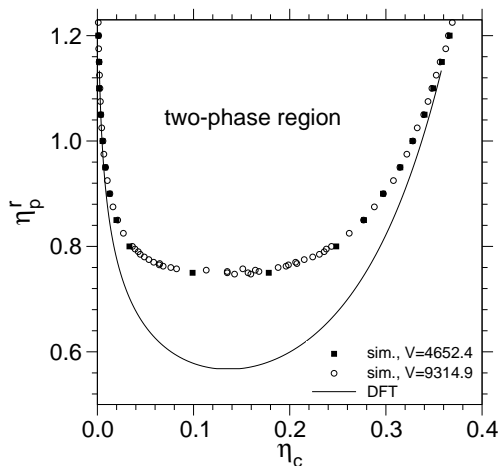


FIG. 2: Phase diagram of the AO model with  $q = 0.8$ . The points are the binodals as obtained from the simulation at the indicated volumes of the simulation box. The solid line is the binodal from DFT [8, 9].

probability distribution  $P(\eta_c)$ . This is the probability of observing a mixture with colloid packing fraction  $\eta_c$ . If phase separation occurs  $P(\eta_c)$  is bimodal: the peak at low  $\eta_c$  corresponds to the colloid vapor phase, the peak at high  $\eta_c$  to the colloid liquid phase, and the region in between is the phase-separated regime. To ensure phase coexistence, the colloid fugacity  $z_c$  is tuned such that the area under both peaks is equal [21].

A crucial point in our simulation is the use of a new biased sampling technique called successive umbrella sampling. This technique was recently developed by Virnau and Müller [18]. Combination of our grand canonical Monte Carlo move and successive umbrella sampling enables us to sample  $P(\eta_c)$  also in regions where, due to the free energy barrier separating both phases,  $P(\eta_c)$  may be very low.

In the following we consider an AO mixture with a polymer to colloid size ratio  $q \equiv R_p/R_c = 0.8$ . Note that all lengths are given in units of  $R_c \equiv 1$ . From previous studies we expect fluid-fluid phase separation for  $q = 0.8$  in a wide range of  $\eta_p^r$ . The simulations were performed in an elongated box with aspect ratio 1/2 and periodic boundary conditions. We have performed simulations for two different volumes of the simulation box:  $V_1 = 4652.4$  and  $V_2 = 9314.9$ . When the colloid packing fraction reaches 0.45, the smaller volume contains 500 colloids and the larger volume 1000 colloids.

Fig. 2 shows the phase diagram for the two system sizes  $V_1$  and  $V_2$ . Comparison of the two data sets shows that finite-size effects are relatively small, even close to the critical point. Also included in Fig. 2 is the phase diagram obtained from recent DFT [8, 9]. We observe that DFT underestimates the location of the critical point by about 30%. More importantly, DFT yields the typ-

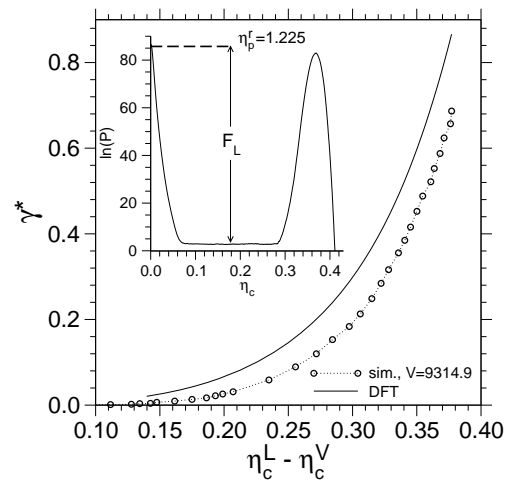


FIG. 3: Reduced interfacial tension  $\gamma^* \equiv 4R_c^2\gamma$  as a function of the difference between the colloid packing fractions in the coexisting liquid (L) and vapor (V) phases. The open circles represent our simulation data. The solid line is a DFT result [20]. The inset shows the logarithm of the probability distribution  $P(\eta_c)$  for  $\eta_p^r = 1.225$  with  $F_L$  defined in the text.

ical mean-field parabolic shape of the binodal (critical exponent  $\beta = 1/2$ ) while the simulation yields the expected flatter binodal ( $\beta \approx 0.325$ ; Ising model universality class [23]). We will demonstrate below that the simulation indeed displays Ising critical behavior.

The probability distribution  $P(\eta_c)$  can also be used to extract the interfacial tension  $\gamma$  between the coexisting colloid vapor and colloid liquid phases. To this end one uses a formula that was first derived by Binder [19]:

$$\gamma \equiv \lim_{L \rightarrow \infty} \frac{F_L}{2L^2} = \lim_{L \rightarrow \infty} \frac{1}{2L^2} \ln \left[ \frac{P^{\max}(\eta_c)}{P^{\min}(\eta_c)} \right], \quad (4)$$

with  $P^{\max}(\eta_c)$  and  $P^{\min}(\eta_c)$  the value of  $P(\eta_c)$  at its maxima and its minimum, respectively, and  $L$  the length of the simulation box parallel to the interface. An example distribution is shown in the inset of Fig. 3 for  $\eta_p^r = 1.225$ . Note that the presence of a flat region between the two peaks is important for an accurate estimate of  $\gamma$ . This is enforced in the simulation by using an elongated box.

Fig. 3 shows the reduced interfacial tension  $\gamma^* \equiv 4R_c^2\gamma$  as a function of the difference between the colloid packing fractions in the coexisting phases, as obtained from our simulation together with a recent DFT result. Again, the DFT result deviates from the simulation by about 30%. This demonstrates that the rather perfect agreement of DFT with experimental data as claimed in Ref. [8] is coincidental. According to our simulation data, the values of  $\gamma^*$  for the AO model underestimate experimental data significantly which shows that more sophisticated models are required to describe colloid-polymer mixtures on a quantitative level.

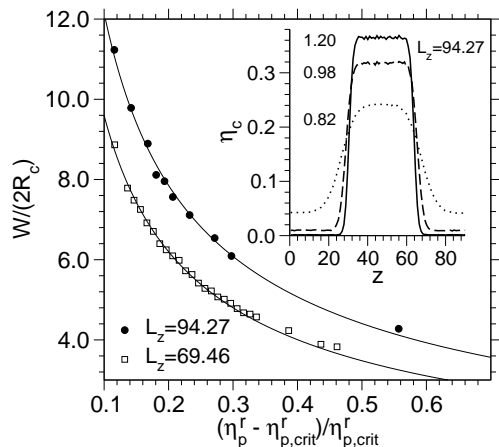


FIG. 4: The width of the colloid interface  $W/(2R_c)$  as a function of the relative distance from the critical reduced polymer packing fraction for two different system sizes as indicated. The solid lines are fits to the 3D Ising power law described in the text. The inset shows three actual colloid density profiles along the direction perpendicular to the interfaces for  $\eta_p^r = \{0.82, 0.98, 1.20\}$ .

We have carried out additional simulations to calculate colloid density profiles in the two-phase region. These simulations were performed using 1156 and 2889 colloidal particles at a colloid packing fraction of 0.13. Periodic boundary conditions were again used and the aspect ratio of both boxes was  $1/3$ . This corresponds to a box length of  $L_z = 69.46$  and  $L_z = 94.27$  for the smaller and larger system, respectively (here  $L_z$  is the box length perpendicular to the interface). Three density profiles for the larger system are shown in the inset of Fig. 4. We have estimated the (10%–90%)-interfacial width  $W$  from these profiles by fitting the profiles to a hyperbolic tangent. Since the interfacial width is expected to diverge with the same exponent as the bulk correlation length near the critical point, one expects  $W \propto (\eta_p^r - \eta_{p,crit}^r)^{-\nu}$ , with  $\nu = 0.63$  corresponding to 3D Ising critical behavior [23]. Fig. 4 shows that the data for both system sizes is consistent with this power law. We can also infer from Fig. 4 that  $W$  depends strongly on  $L_z$ , even far away from the critical point. This is most likely due to capillary waves [24] and care has to be taken when comparing  $W$  from this simulation to interfacial widths obtained in experiments or analytical theories.

In summary, we have presented a grand canonical Monte Carlo method which is well suited to simulate asymmetric binary mixtures. It is particularly powerful when combined with a re-weighting scheme: both the phase diagram and the surface tension can be obtained accurately in that case. We have used the method to determine the coexistence line of the fluid–fluid transition in the AO model with high accuracy. We have also pre-

sented new analysis of the interface between coexisting phases in the AO model, in particular estimates of the interfacial tension.

We are grateful to the Deutsche Forschungsgemeinschaft for support (TR6/A5) and to K. Binder, M. Müller, M. Schmidt and P. Virnau for stimulating discussion.

- 
- [1] S. Asakura and F. Oosawa, J. Chem. Phys. **22**, 1255 (1954).
  - [2] A. Vrij, Pure Appl. Chem. **48**, 471 (1976).
  - [3] A. Vrij, Physica A **235**, 120 (1997).
  - [4] D. G. A. L. Aarts, R. Tuinier, and H. N. W. Lekkerkerker, J. Phys.: Condens. Matter **14**, 7551 (2002).
  - [5] R. Roth, R. Evans, and S. Dietrich, Phys. Rev. E **62**, 5360 (2000).
  - [6] J. L. Lebowitz and J. S. Rowlinson, J. Chem. Phys. **41**, 133 (1964); J. L. Barrat, M. Baus, and J. P. Hansen, Phys. Rev. Lett. **56**, 1063 (1986); T. Biben, P. Bladon, and D. Frenkel, J. Phys.: Condens. Matter **8**, 10799 (1996); M. Dijkstra, R. van Roij, and R. Evans, Phys. Rev. E **59**, 5744 (1999).
  - [7] J. M. Brader and R. Evans, Europhys. Lett. **49**, 678 (2000).
  - [8] J. M. Brader, R. Evans, M. Schmidt, and H. Löwen, J. Phys. Condens. Matter **14**, L1 (2002).
  - [9] M. Schmidt, H. Löwen, J. M. Brader, and R. Evans, Phys. Rev. Lett. **85**, 1934 (2000).
  - [10] E. H. A. de Hoog and H. N. W. Lekkerkerker, J. Phys. Chem. B **103**, 5274 (1999).
  - [11] B.-H. Chen, B. Payandeh, and M. Robert, Phys. Rev. E **62**, 2369 (2000).
  - [12] M. Dijkstra and R. van Roij, Phys. Rev. E **56**, 5594 (1997).
  - [13] P. G. Bolhuis, A. A. Louis, and J-P. Hansen, Phys. Rev. Lett. **89**, 128302 (2002).
  - [14] A. Z. Panagiotopoulos, Mol. Phys. **61**, 813 (1987).
  - [15] T. Biben, P. Bladon, and D. Frenkel, J. Phys.: Condens. Matter **8**, 10799 (1996).
  - [16] A. Buhot and W. Krauth, Phys. Rev. Lett. **80**, 3787 (1998).
  - [17] F. Varnik, J. Baschnagel, and K. Binder, J. Chem. Phys. **113**, 4444 (2000).
  - [18] P. Virnau and M. Müller, submitted (2003), preprint cond-mat/0306678.
  - [19] K. Binder, Phys. Rev. A **25**, 1699 (1982).
  - [20] M. Schmidt, private communication (2003).
  - [21] D. P. Landau and K. Binder, *A Guide to Monte Carlo Simulations in Statistical Physics* (Cambridge University Press, Cambridge, 2000).
  - [22] M. E. J. Newman and G. T. Barkema, *Monte Carlo Methods in Statistical Physics* (Clarendon Press, Oxford, 1999).
  - [23] E. Luijten and K. Binder, Phys. Rep. **344**, 179 (2001).
  - [24] K. Binder and M. Müller, Int. J. Mod. Phys. C **11**, 1093 (2000).